Application of quantum cascade lasers to high-precision atmospheric trace gas measurements

Application of quantum cascade lasers to high-precision atmospheric trace gas measurements

J. Barry McManus, MEMBER SPIE
Mark S. Zahniser
David D. Nelson, Jr.
Joanne H. Shorter
Scott Herndon
Ezra Wood
Aerodyne Research, Inc.
Center for Atmospheric and Environmental Chemistry
45 Manning Road
Billerica, Massachusetts 01821
E-mail: mcmanus@aerodyne.com

Rick Wehr
The University of Arizona
Department of Ecology and Evolutionary Biology
Tucson, Arizona 85721

Abstract. We review our recent results in development of high-precision laser spectroscopic instrumentation using midinfrared quantum cascade lasers (QCLs). Some of these instruments have been directed at measurements of atmospheric trace gases where a fractional precision of 10^{-3} or better of ambient concentration may be required. Such high precision is needed in measurements of fluxes of stable atmospheric gases and measurements of isotopic ratios. Instruments that are based on thermoelectrically cooled midinfrared QCLs and thermoelectrically cooled detectors have been demonstrated that meet the requirements of high-precision atmospheric measurements, without the need for cryogens. We also describe the design of and results from a new dual QCL instrument with a 200-m path-length absorption cell. This instrument has demonstrated 1-s noise of 32 ppt for formaldehyde (HCHO) and 9 ppt for carbonyl sulfide (OCS).
[DOI: 10.1117/1.3498782]

Subject terms: quantum cascade lasers; laser spectroscopy; atmospheric chemistry.

Paper 100364SSR received Apr. 24, 2010; revised manuscript received Jul. 30, 2010; accepted for publication Aug. 2, 2010; published online Dec. 2, 2010.

1 Introduction

The invention of quantum cascade lasers (QCLs)[1–6] has been pivotal in the recent development of high-precision midinfrared (mid-IR) spectroscopic instrumentation for atmospheric trace gas measurements.[7–27] Instruments based on QCLs have been deployed in field settings to help answer questions posed in atmospheric chemistry research. There has been great progress in moving from cryogenically cooled QCLs[9,10] and detectors, to thermoelectrically (TE)-cooled QCLs, and more recently with fully cryogen-free systems employing TE-cooled detectors.[11–24] Further improvement in performance has been achieved with the advent of CW QCLs.[2,3,6,25–27] Both high-sensitivity and high-precision measurements of trace gases have been demonstrated. Relevant concentrations of atmospheric trace gases extend into the parts-per-trillion (ppt) range, and needs for precision in the ratios of gases may be on the order of one part in 10^4. In this paper, we review development of QCL laser-based instrumentation at Aerodyne Research, Inc. (ARI)[15–27] and will present results from a new instrument.

Atmospheric trace gas measurement problems cover a range of requirements in terms of sensitivity, precision, speed, and specificity. The measurement requirements also must be balanced by system cost, which includes the costs of instrument construction as well as operation and interpretation of data. Low-cost and low-performance sensors are sufficient for applications such as carbon monoxide (CO) monitors for the home. Higher performance is needed for routine pollution monitors. Pollution monitors also need to work unattended for long periods and to have costs that are consistent with the establishment of large networks. The highest performance requirements are presented by the needs of atmospheric chemistry research. In atmospheric chemistry research, the questions and challenges evolve as the science develops. There is a trend toward resolving questions involving chemicals at very low mixing ratios (on the order of 10^{-12} mole trace gas/mole air, i.e., ppt levels) and toward precision measurements at high speed. Another important aspect of atmospheric chemistry instrumentation is the need to operate in a field site, on fixed or mobile platforms, with variable temperature, pressure, and acceleration.

Infrared (IR) laser spectroscopy,[28,29] which has been useful for many years as a laboratory tool, is also an excellent method for trace gas analysis in atmospheric research. By focusing on one or a small set of absorption lines, rapid high-sensitivity measurements can be achieved. Laser spectroscopic measurements are highly specific, with little influence from other trace gases (which can be a serious problem for mass spectrometer-based measurements). IR laser spectroscopy also is becoming more useful for applications requiring high-precision measurements (i.e., to distinguish small changes in concentration). In making high-precision trace gas measurements with laser spectroscopy, there are several basic issues in common with high-sensitivity measurements and several distinct issues. In common with high-sensitivity measurements, high precision requires low detector and laser noise, and low interference from other substances. Distinct from high-sensitivity measurements, high-precision measurements have the additional requirements of stable scale factor, high degree of linearity, and low noise associated with the nominal concentration.

QCL, first announced in 1994,[1–6] were the first mid-IR semiconductor lasers that did not require cryogenic cooling. Thus, QCLs opened the door to truly field-ready mid-IR instrumentation. The first QCLs to be commercially available operated in pulsed mode, and most available QCLs still do. Pulsed-mode operation has drawbacks for precision measurements, such as broader and asymmetrical line shape

0091-3286/2010/$25.00 © 2010 SPIE

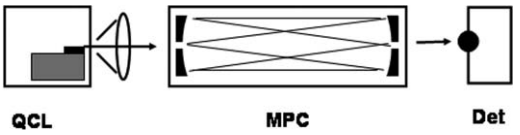

Fig. 1 Schematic diagram of a very simple spectrometer with a single QCL, a MPC and a detector (Det). The QCL is mounted on a thermoelectric cooler in a hermetic enclosure, and a lens or other optical element is used to collect the widely divergent light into a narrow beam.

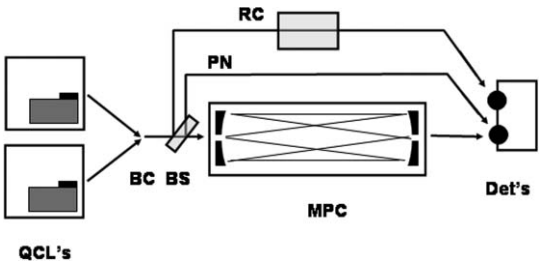

Fig. 2 Schematic of a more complex spectrometer, with two QCLs. Their beams are combined (BC) and most of the light goes through a MPC and to a detector (Det). Before the MPC, a beamsplitter (BS) directs a fraction of the light through a reference cell (RC) and to a power-normalization (PN) path.

and pulse-to-pulse energy variations. Despite these drawbacks, high-precision measurements have been achieved using pulsed lasers.[11–13,15–24] QCLs that operate continuously at near room temperature have recently become commercially available. Continuous wave (CW) operation of QCLs has led to improved precision in some cases.[25–27] There are several reasons for the improvement, including narrower line width, which produces deeper and more symmetrical absorption features. Also, the average power is higher than in pulsed lasers, which leads to improved signal-to-noise ratio (SNR) with thermoelectrically cooled detectors. CW operation also leads to less variation in laser power.

In this paper, we review the development of QCL-based instruments at ARI, especially those instruments with applications in atmospheric chemistry research. Also, we will concentrate on instruments with the highest performance in terms of sensitivity and precision. Sections 2–4 explain the general characteristics of QCL-based trace gas instruments at ARI, followed by several examples of specific instruments. Finally, we will describe our latest instrument and present measurement results.

2 General Characteristics of QCL-Based Trace Gas Instruments at ARI

Combining mid-IR QCLs with the techniques of long path-length absorption spectroscopy provides a flexible and straightforward route to high-sensitivity and high-precision measurements of a wide variety of gas-phase molecules. Increasing the absorption path length is a universal method of increasing the absorption depth and, thus, the sensitivity of spectroscopic measurements. For strongly absorbing gases at high concentrations, a few millimeters of path may be sufficient, but some measurement problems require a path length of hundreds of meters. Low pressure (typically, ~1/20 atmosphere) yields narrow absorption lines for maximum sensitivity and minimum interference from other gases. The long path length generally is provided by a multipass cell, an optical device to fold the path into a compact volume. The astigmatic Herriot cell configuration is used in most of the instruments designed at ARI.[30,31]

The basic configuration of a long-path length spectrometer is quite simple. There is a laser, followed by a multipass cell and then a detector. A schematic drawing of such a configuration is shown in Fig. 1. The multipass cell (MPC) has a definite path length, and a considerable fraction of the laser light may be transmitted to the detector, minimizing the effects of detector noise. The basic measurement of the absorption involves a comparison of three quantities, the signal at zero light, the signal due to background light (on either side of the absorption), and the light signal centered on the absorption line. Ideally, one should measure the area of the absorption line (i.e., the integrated deviation of the light signal from background). To measure the absorption line, the laser may be linearly scanned over the line to observe the direct absorption shape or it may be modulated sinusoidally to produce signals that are analyzed in terms of harmonic content. Although either method can yield low-noise measurements (as long as the sweep or modulation frequency is high enough to avoid low-frequency laser flicker noise), there are advantages to the direct absorption-sweep integration method in terms of ease of area integration and higher spectral resolution.

In practice, the configuration of a long-path length spectrometer tends be more complicated than what is shown in Fig. 1. For example, two or more lasers may be combined to pass through the cell. A fraction of the laser output may be split from the main beam for diagnostic or control purposes. Monitoring the laser output power allows one to reduce the effects of power variations with normalization, which is particularly beneficial with pulsed QCL operation. If a fraction of the laser output passes through a short cell containing a high concentration of the gas of interest, then the laser frequency may be locked to a specific absorption line. A schematic diagram of a more complex spectrometer is shown in Fig. 2, and a photograph of the corresponding completed instrument is shown in Fig. 3.

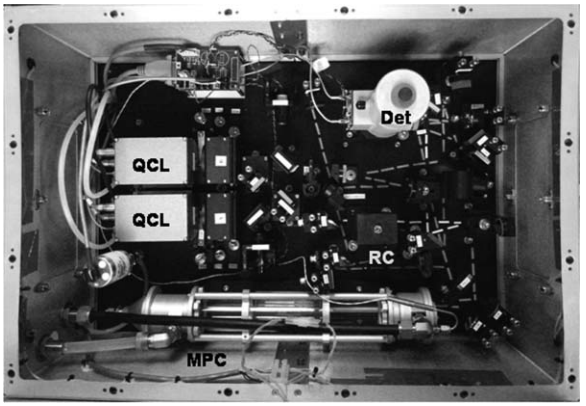

Fig. 3 Photograph of a dual quantum cascade laser spectrometer used for atmospheric research. The pulsed QCLs are in blue housings. Beams from the two lasers are combined to pass through a sample MPC with 76-m path length. A small fraction of the combined beam is split off to go through a short RC. Another split-off path is used for power normalization. All three optical paths end at a pair of liquid-nitrogen–cooled detectors in a single dewar (Det).

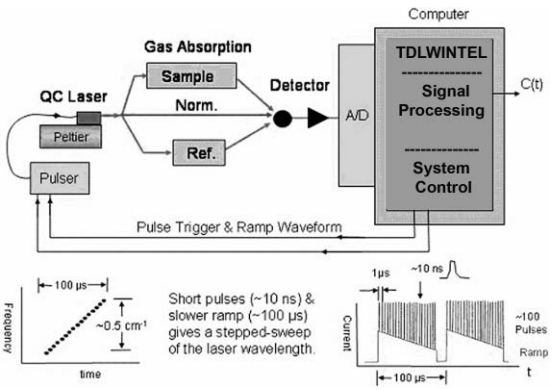

Fig. 4 Schematic diagram of the laser sweep and signal processing system for a pulsed QCL instrument.

Our general approach to atmospheric trace gas measurements is to use tunable IR laser differential absorption spectroscopy with rapid laser frequency sweeps[15] and long-path, multiple-pass absorption cells[30,31] to obtain absorption spectra with a high SNR. The laser is repeatedly swept at high frequency (~1–5 kHz) across a narrow spectral range (~0.5 cm^{-1}), with a shutoff period (to measure laser power) at the end of each sweep. The data analysis program TDLWINTEL[15] controls laser sweep, data acquisition, and analysis. Detected signals are synchronously averaged and then fit, using HITRAN[32] parameters with measured pressure and temperature to determine mixing ratios. The same control and analysis program can be used for either pulsed or CW lasers.

Our spectral analysis method has been developed with the goal of providing both high sensitivity and high stability. This approach is tolerant of small drifts in laser frequency, which may be difficult to completely suppress. The line center is continuously determined by the fit, using spectra from either a reference cell or the main sample cell. In addition, a feedback system adjusts the laser base temperature based on the measured line center, which can yield laser frequency stability on the order of 1 MHz. The laser frequency stability usually is limited by the control electronics and thermal delays. At the present level of control, laser frequency stability is seldom the limiting factor in sensitivity. The fitting also can determine the effective laser line width, but in practice, we only need to determine the line width at setup and do not adjust it in real time.

In Fig. 4, we show a schematic representation of the data acquisition system and its interface with the key optical components (the laser, the detector, and the long-path absorption cell). This diagram is specific to pulsed laser systems. At the center of Fig. 4 is the computer and the data acquisition card, a National Instruments PCI6111E board, which generates three synchronized signals: (i) a high-frequency (typically, 1 MHz) transistor-transistor logic (TTL) pulse train to trigger the pulse electronics which drive the laser above threshold, (ii) a TTL enabling gate that defines the duration of a single spectral sweep (typically, 100 μs with the gate enabled 90% of the time), and (iii) an analog voltage ramp (also 100-μs duration), which is used to create a subthreshold laser current to rapidly scan the laser via temperature tuning. The enabling gate turns off the pulse train at the end of each sweep to measure the detector offset voltage. The sweep waveform typically consists of a series of sharp current spikes superimposed on a declining baseline. The amplitude of each pulse is typically several amps, and its duration is 10–15 ns. To improve the stability of the output current, the entire module is temperature stabilized to ± 0.1°C using a temperature-controlled recirculating fluid (75% water, 25% ethanol). This same fluid is also directed to the laser's Peltier cooler to remove its waste heat. The arrangement of the optical paths is similar to that shown in Fig. 2. The 76-m multipass sample cell produces a delay (250 ns) between arrival times of the reference and sample pulses at the detector, which allows one to separately capture the pulses with the 5-MHz data acquisition card.

We frequently use a power normalization technique to account for laser amplitude noise.[15,17] A beamsplitter generates an optical path that does not pass through the sample MPC to produce a normalization spectrum. Each sample spectrum is divided by the corresponding normalization spectrum before spectral analysis. This procedure produces a normalized sample spectrum with a much flatter baseline and with considerably reduced laser amplitude noise, especially when using pulsed lasers.

3 Optics Approaches

In the several QCL-based instruments we have designed, there are a set of common approaches to the optical designs, which are driven by a set of general requirements and expectations. Our research instruments are intended for field use; thus, the designs must be robust enough for use in motion or at a field site with poor environmental control. Having experienced and involved operators allows for a degree of complexity that helps to achieve the highest performance. The same design may be adapted to study different gases, with a change of laser(s) and possibly of detector(s). Methods of alignment are built into the designs.

For maximum flexibility in choice of wavelength, the optical designs are largely based on reflective optics. This allows changing lasers and also coalignment of trace lasers to visualize the optical path. For focusing elements, we often use spherical mirrors at close to normal. Spherical mirrors reduce cost and are readily available. The aberrations introduced by spheres at low off-axis angle are generally tolerable and may be compensated for, to some degree, with pairs of spherical reflectors at specific angles. For the more demanding imaging problem of transforming the low *f*-number output cone from the laser to a higher *f*-number beam, we use Schwarzschild reflecting objectives. These objectives have the advantages of good optical quality and a wide field of view, although with the drawbacks of large size and high cost. They also offer the option of viewing the laser face directly, by placing an eyepiece in the optical path. Indeed, the capability of viewing the laser directly at high magnification is extremely useful when replacing and aligning lasers.

The problem of aligning the IR beam can be made relatively simple when alignment aids are built into the system. The starting point for alignment in the design is to establish a pinhole aperture as the "optical anchor" for the instrument. The QCL is first imaged through the pinhole, into the MPC, and then onto the detector. A visible trace laser is also imaged through the pinhole and thus follows a path that is similar to that of the IR laser and forms a similar image at the detector. An eyepiece placed at the pinhole position allows a

clear view of the laser, and the laser can be placed at the center of the field of view during setup, which is close to the position needed for imaging through the pinhole. A more precise method of positioning the laser is to direct a trace laser backward through the pinhole to form an image on the laser face. With these steps, we can replace a laser and find the IR signal almost immediately. Although the pinhole is extremely useful for alignment, it is moved out of the beam for operation of the instrument to avoid generating interference fringes from light reflecting back to the laser.

Although MPCs may be used to increase the optical path length through a sample of gas, and thereby increase the measurement sensitivity, the design of MPCs involves a trade-off between minimizing volume and minimizing interference fringes. Minimizing the cell volume is important to reduce the overall instrument size and to reduce the amount of time and energy needed to exchange gas. Because many multipass cells are operated at reduced pressure (to reduce pressure broadening), reducing the volume reduces the size of the pump, which can be a large part of the system power requirement. Scattering of light at the input or output points, or on the mirror surfaces, can cause some light to exit the cell early or late and interfere with light following the main path. Interference fringes produced by scatter-induced path-length differences often limit the achievable SNR improvement available from MPCs. Interference fringes can be reduced by making the mirrors larger to more widely separate beam spots, thereby increasing the cell volume. Various other methods can be used to reduce interference fringes, such as designing the circulation pattern to minimize fringes near the absorption line-width, vibrating the mirrors to average fringes, and keeping the mirrors clean to minimize scatter. Improving mirror reflectivity may also lead to lower fringes by reducing the ratio of scattered light to transmitted light. Recent advances in mid-IR optical coatings allow reflectivity of >0.998 for each reflection.

The astigmatic multipass absorption cell (AMAC) is a configuration that was developed as a practical device at ARI.[30,31] We have a set of AMAC designs that are used in our tunable laser instruments. These cells offer long, well-defined absorption path length (18–210 m) with good optical throughput and relatively small gas volume. The AMAC architecture uses two mirrors, both with two different radii of curvature (Fig. 5). Light that is injected through a hole in the front mirror reflects back and forth between the mirrors hundreds of times before exiting through the front-mirror hole. The light exiting the cell is separated in angle from the input beam. The specific circulation pattern of light through the cell is determined by the radii of curvature of the mirrors, and by the spacing and axial-twist angle of the mirrors. ARI has developed a comprehensive theoretical model of the operation of the cells, which allows one to predict available patterns and their characteristics.

4 Examples of QCL-Based Instrument Designs

Several instrument optical configurations have been developed at ARI for different measurement problems. The most commonly used configurations are a compact single-laser system,[21] a dual-laser system,[18,19] and a CO_2 isotope system with a single laser and two matched optical cells.[22–24] The first two systems have a measurement path with a 76-m multipass cell and two other diagnostic paths that are used for power normalization and laser frequency locking. The CO_2 isotope system uses a pair of matched 7-m path-length cells, for the sample and a reference gas. All these systems can use thermoelectrically cooled mid-IR detectors.

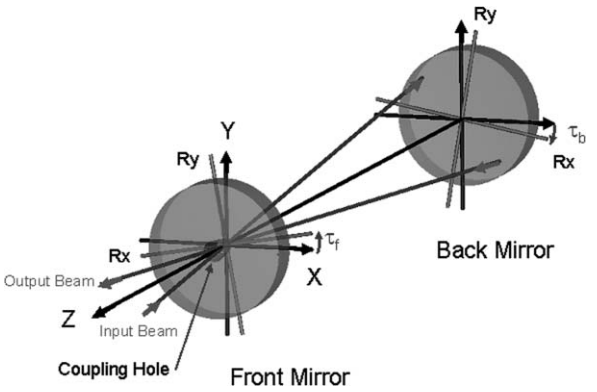

Fig. 5 Astigmatic Herriott cell geometry. Light enters and exits through a front mirror hole, with separation by angle. Front and back mirrors have two radii of curvature, R_x and R_y. Circulation patterns are selected by adjusting mirror spacing and twist of the mirrors about the center axis.

4.1 *Compact-Single Laser Instrument*

The compact single QCL instrument has been used for sensitive, rapid, and continuous measurement of trace gases in air, such as methane (CH_4), nitric oxide (NO), nitrous oxide (N_2O), and ammonia (NH_3).[21] The single QCL may be substituted to measure the various gases. The instrument operates continuously, requiring little operator attention, and Web-based remote access is provided for instrument control, calibration, and data retrieval. The instrument design includes a TE-cooled pulsed or CW distributed feedback (DFB) QCL, a low-volume (0.5 l) MPC offering 76-m absorption path length, and a TE-cooled detector. A photograph of the instrument is shown in Fig. 6. The instrument has been applied to field measurements of various gases of environmental concern.

This high sensitivity fully noncryogenic design, which operates as far into the IR as the 10-μm region is made possible by advances in laser and detector technology. The light source is a mid-IR TE-cooled pulsed QCL with a DFB grating [Alpes Laser, Neuchatel, Switzerland]. The

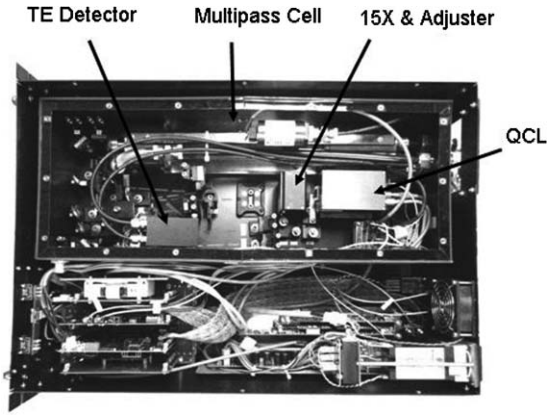

Fig. 6 Photograph (top view) of the compact single-laser instrument. The optical table is in the upper section, and the electronics are in the lower section.

Table 1 Summary of noise performance achieved with a single-QCL instrument with a 76-m multipass absorption cell.

Measured Gas		1-Hz Conc. Noise, ppb	Allan Variance Min sdev & time
CH_4		1.0	0.2 at 100 s
NO		0.3	0.05 at 200 s
N_2O	(2243 cm^{-1})	0.16	0.03 at 160 s
N_2O	(1271 cm^{-1})	0.38	0.033 at 400 s
NH_3		0.2	0.02 at 100 s

detector is TE cooled. For the shorter laser wavelengths, we typically use either a HgCdTe photodiode (nonimmersed) or a HgCdZnTe photodiode with an immersion lens. For the 10-μm region, we typically use a photoconductive detector with an immersion lens [Vigo Systems, S. A. model no. PCI-3TE-10.6], with D^* at 10 μm of 5×10^9 cm W^{-1} $Hz^{1/2}$. TE-cooled detectors with higher values of D^* are available for species that can be monitored at shorter wavelengths. D^* values of at least 2×10^{10} cm W^{-1} $Hz^{1/2}$ can be obtained at 5 μm. Waste heat from the TE coolers is removed with circulating water/ethanol at constant temperature. A summary of the short- and long-term noise is given in Table 1.

4.2 *Dual-Laser Instrument*

By combining the beams from two QCLs onto a single path through a MPC, we extend our capabilities for simultaneous measurement of multiple trace gases. The dual-laser spectrometer shown in Fig. 3 is part of an instrument suite developed jointly at Harvard University and ARI.[18,19,33] This particular instrument has two pulsed, thermoelectricaly cooled QCLs, one operating at 7.8 μm to measure CH_4 and N_2O and another at 4.6 μm to measure CO. As in the compact single-laser instrument, the (astigmatic Herriott) multipass absorption cell in this instrument has 76 m of path in a volume of 0.5 l. The detectors in this instrument are liquid nitrogen cooled for maximum performance. The demonstrated precision at 1 Hz is 0.2 ppb for CO, 0.8 ppb for CH_4 (1 part in 2000 of ambient), and 0.1 ppb for N_2O (1 part in 3000 of ambient).

The dual QCL spectrometer described above has been integrated into an instrument suite aboard the NSF HIAPER research aircraft and has already flown on several missions sampling the atmosphere (nearly) from pole to pole. The Harvard University (Steve Wofsy Group) instrument also contains a second QCL instrument for measuring CO_2. For the CO_2 instrument, a precision of 1 part in 10,000 of ambient (30 ppb in 1 s) is achieved with only ~15 cm absorption path length. The recently completed first sampling mission, with the code name "HIPPO," for "Hiaper pole-to-pole observations of carbon cycle and greenhouse gases," has produced the most comprehensive profile of a suite of greenhouse gases from the boundary layer to the lower stratosphere and from the south Pacific to the high Arctic [HIPPO]. Continuing HIPPO flights will help to constrain global models of greenhouse gas sources, sinks, and transport.

With our dual-laser instrument, the short-term noise (1 s average) in ambient N_2O is typically 0.3–0.5 ppb with a pulsed laser, and 0.15–0.25 ppb with a CW laser. Thus, the CW laser offers improved short-term noise, with fractional precision of $>10^{-3}$ (e.g., with a N_2O noise level of <0.3 ppb compared to an ambient concentration of 320 ppb). However, with longer averaging (30–100 s) both the pulsed and CW laser instruments reach a similar limiting noise level of 0.02–0.06 ppb. The long-term noise performance with a CW laser is not systematically better than with a pulsed laser because other noise and drift effects, which are common to both types of laser, begin to dominate. Those effects, such as line-width variations and instability of the laser line position, are stronger when there is a significant absorption depth. For CW lasers, with inherently narrower line width, such stability issues are more of a concern than with pulsed lasers. Thus, effects other than the laser or detector noise dominate in precision measurements of gases for which there is an appreciable ambient concentration.

4.3 *CO_2 Isotopes Instrument*

Measurement of isotopic ratios of trace gases in ambient air presents an extreme challenge of precision. For the ratio of $^{13}CO_2$ to $^{12}CO_2$, both isotopologues must be measured with a precision on the order of 10^{-4} to be useful in environmental questions. Because CO_2 has a significant minimum atmospheric concentration (~380 ppm), noise and drift sources that are proportional to the gas concentration limit the available precision. We alleviate that problem by measuring the sample and a reference gas in nearly identical absorption cells and dividing the spectra before deriving concentrations. Dividing the spectra effectively cancels most of the absorption depth and reduces the effect of associated drift sources. With this technique, we have previously demonstrated a measurement precision for three isotopologues of CO_2 of 0.2‰ in 1 s and 0.02‰ in 400 s with a pulsed QCL spectrometer and a LN2-cooled detector.[22–24] When a CW QCL is used in the same instrument design, with thermoelectrically cooled detectors, we achieve twice the previous short-term precision. Sampling laboratory air in both cells, the short-term (1 s) standard deviation in isotopic ratio is ~0.12‰, and a minimum standard deviation (with ~100-s average) is 0.025‰. These are claimed to be the most precise isotope ratio measurements with a spectroscopic system that have been reported to date.

4.4 *New Dual QCL Instrument with 200-m Absorption Cell*

ARI has recently developed a new dual QCL trace gas instrument that has shown significant improvements in sensitivity and precision. The instrument has a 200-m path-length multipass cell, with an overall length of ~60 cm. The design is enabled by the availability of high-reflectivity mirror coatings(>99.8%), which makes a cell with >400 passes useful. The design is also enabled by the availability of CW QCLs, with high-enough power to overcome the dark noise limits of TE-cooled detectors. The instrument may be used to measure a variety of trace gases, depending on the choice of lasers and detectors, as well as the reflectivity curve for the multipass cell. In the version of the instrument described here, one CW-QCL operates near 1765 cm^{-1} and measures H_2O, formaldehyde (HCHO), and formic acid (HCOOH).

The other CW-QCL operates near 2052 cm^{-1} and measures CO_2 and carbonyl sulfide (OCS). The gases of primary interest in the measurement, HCHO and OCS, have been measured previously with QCLs or other lasers.[19,34–40] The choice to measure these gases is driven by an upcoming field-measurement campaign.

The optical design of the new dual instrument is based on our previous dual instrument with a 76-m cell, with several innovations that allow placement of a new 200-m cell on the 43×64 cm table. A schematic diagram of the layout is shown in Fig. 7. The optical train begins with the two QCLs mounted on Peltier coolers in sealed housings. Laser light is collected by a pair of 15X Schwarzchild objectives, then combined with a dichroic beamsplitter and focused through a pinhole. The objectives are moved to adjust their images with custom-built translators based on stacked kinematically indexed plates. The segment of the optical train before the pinhole has several alignment aids built in. A visible trace laser, which is coaligned with one of the IR laser beams, allows visualizing the optical path all the way to the detector. Both IR beams reflect from visible-IR dichroics, which allows one to have viewing points for both lasers. A drop-in eyepiece placed behind the dichroics, combined with the 15X objectives, gives 150X views of the laser faces. Past the pinhole, the combined beam is reimaged into the MPC in two steps, which increases the magnification and thus reduces the beam angle.

We aim the high F#IR beam into the cell using a particular arrangement that allows independent aiming through the entrance hole and onto the back mirror, without either adjustment influencing the other. A focusing mirror is placed before the cell entrance at a distance to produce images of the back mirror and input hole on the two upstream adjustment mirrors. Adjusting the laser beam direction on the mirror with either image leaves the position of the beam stationary on the imaged optic. Thus, we may adjust aiming at the input hole with the mirror where the back cell mirror is imaged, without affecting the beam position on the back mirror. Similarly, we may adjust aiming at the back cell mirror with the mirror where the input hole is imaged, without affecting the beam position on the input hole. This

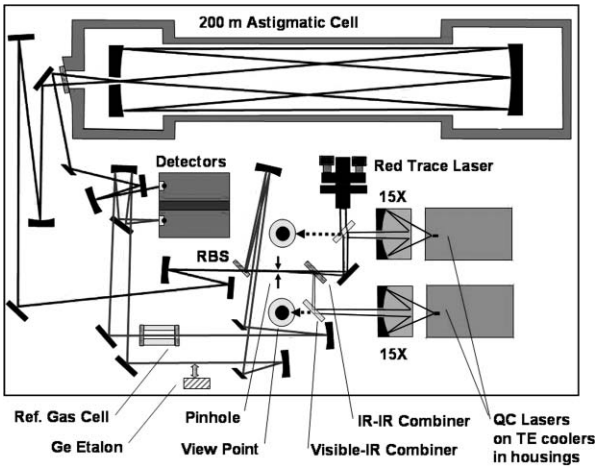

Fig. 7 Schematic diagram of our new instrument. The optical table measures 43×64 cm, and has two TE-cooled CW DFB-QCLs at 1765 cm^{-1} (5.66 μm) and 2052 cm^{-1} (4.87 μm) for measuring HCHO and OCS, respectfully. The first beam forming is with 15x Schwarzchild objectives. The two laser beams are combined with a dichroic beamsplitter (IR-IR combiner). The main path has a 200-m path-length sample cell. Two reference paths are formed by reflection from a BaF_2 beamsplitter (RBS).

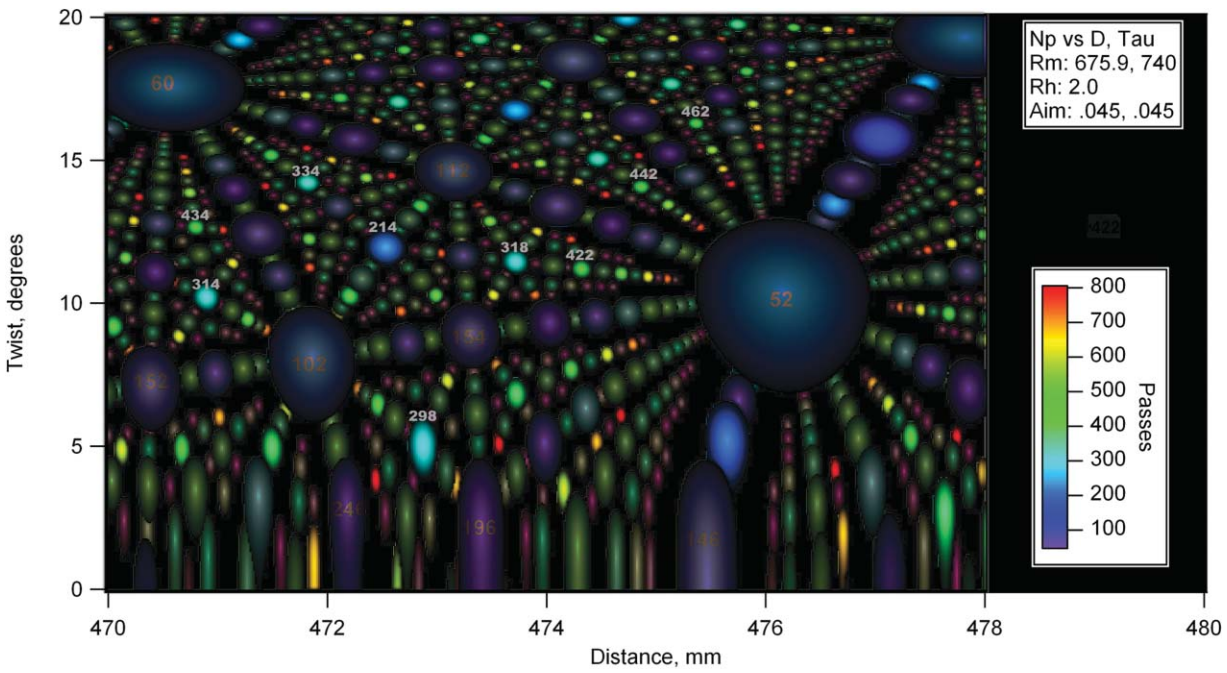

Fig. 8 Map of pattern locations as a function of mirror spacing and twist, for a range of setup conditions close to the desired pattern with 422 passes (near center). The map is calculated using nonparaxial ray tracing with a single ray at a finite angle. The map shows nearly circular zones, each representing the location of a different pattern. The pass number is indicated by color. The error in the return location of the final ray is indicated by the darkened tone at the edge of each zone. The patterns with the beam exiting in the wrong direction (incomplete patterns) are indicated with a grayer color.

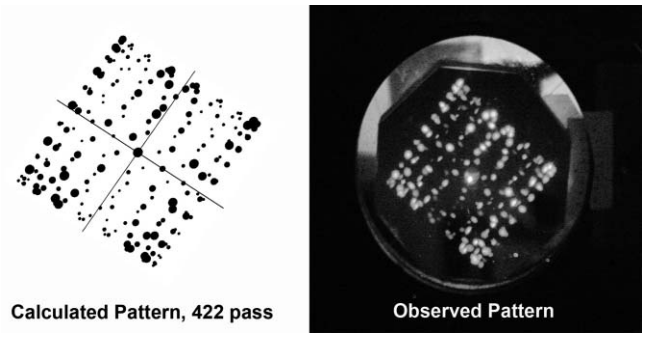

Fig. 9 Simulated and actual mirror spots for the 422-pass pattern in the astigmatic Herriott cell.

arrangement greatly simplifies optimizing the beam coupling into the cell.

The dual laser instrument has two reference paths, derived from reflection from the two faces of a wedged beamsplitter. There is a "reference-locking" path that contains one or two short gas cells with high concentrations of the gases of interest. Fitting to absorption lines produced by the gas cell allows one to lock the laser frequencies to specific absorption lines. The other reference path may be used for power normalization, or a Ge etalon may be flipped into the path in order to measure the laser tuning rate. An electromagnetically actuated flag may be flipped to allow either reference beam to reach the single reference detector.

The new 200-m path-length (422-pass) astigmatic cell is an extension of earlier designs, with the same underlying concepts as presented earlier, but with twice as many passes and with an optomechanical design allowing easier mirror removal or replacement. The cell has 7.8-cm-diam toroidal-surface mirrors at a separation of 47.4 cm, giving an active volume of 2.1 l. The high number of passes is made possible by newly available mid-IR high-reflectivity coatings. Another challenge in setting up this cell is to navigate to the specific high-pass number pattern that we want. That navigation is made possible with a computed map of the patterns as a function of mirror spacing and twist, as shown in Fig. 8. In Fig. 9, we show the simulated 422-pass beam-spot pattern

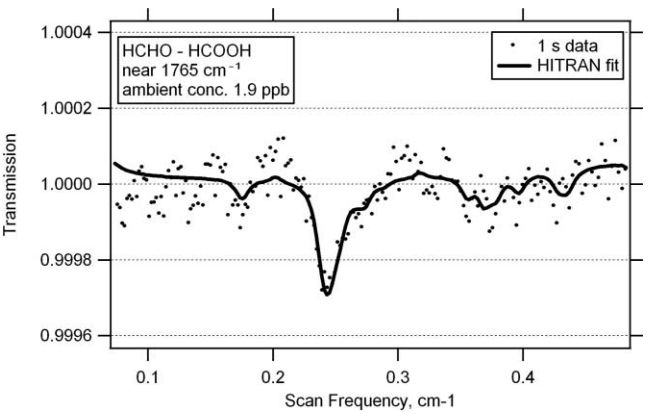

Fig. 10 Transmission spectra with 1-s averaging for ambient air containing 1.9 ppb formaldehyde. Dots are the acquired data and solid lines are fits based in HITRAN data and measured parameters (cell pressure and temperature).

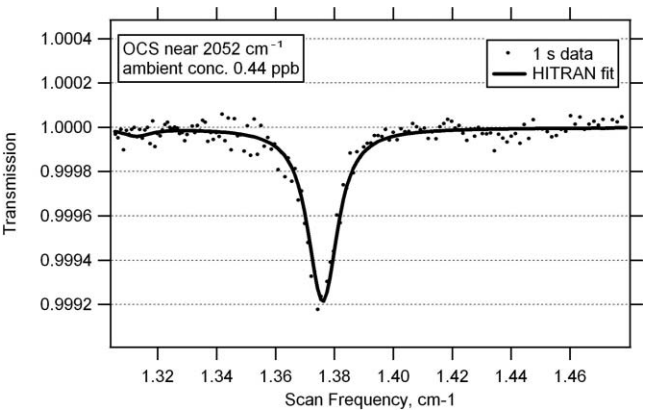

Fig. 11 Transmission spectra with 1-s averaging for ambient air containing 0.44 ppb carbonyl sulfide. Dots are the acquired data, and solid lines are fits based in HITRAN data and measured parameters (cell pressure and temperature).

on the front mirror, and a photograph of the actual pattern seen with a 670-nm trace laser.

Among our best instrument performances to date have been demonstrated with the new dual-laser design. We have tested the instrument with both TE-cooled and LN2-cooled detectors. For the data presented next, we used the LN2 detector. The short-term noise with the TE-cooled detectors was similar to that achieved with the LN2 detector, but the LN2 detector had better stability and less saturation, which gave better results in terms of absolute concentrations. Examples of 1-s-averaged transmission spectra for HCHO and OCS at ambient concentrations are shown in Figs. 10 and 11, along with fits based on HITRAN and measured parameters. When these spectra were acquired, the ambient concentration for HCHO was 1.9 ppb and the ambient concentration for OCS was 0.44 ppb. The absorption strength for OCS is approximately ten times that of HCHO. In Fig. 12, we show an Allan variance plot for a measurement of formaldehyde in a sample gas containing near-zero concentration. Background spectra were collected every 10 min, for subtraction from subsequent measured spectra. The 1-s HCHO concentration noise is

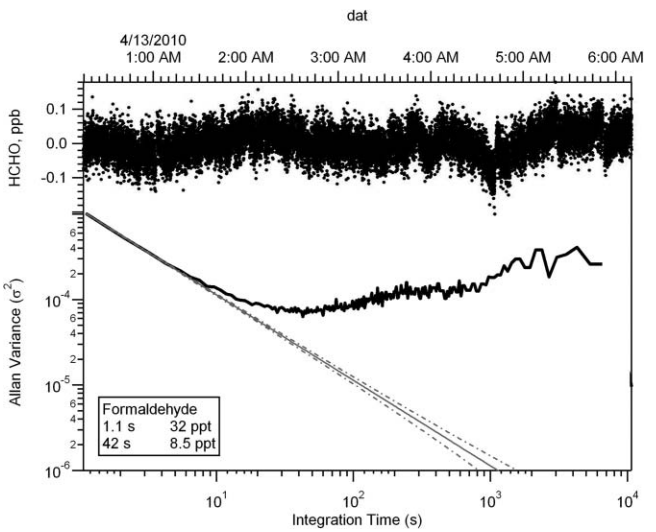

Fig. 12 Allan variance plot for HCHO measured with the dual laser instrument in the laboratory, with "zero" air.

Table 2 Summary of noise results for the dual laser instrument with a 200-m cell.

		Allan Variance Min.	
Measured Gas	1-s Noise (ppt)	Time (s)	Noise (ppt)
HCHO	32	42	8.9
HCOOH	50	30	17
OCS	9.2	30	2.9

32 ppt. At the Allan variance[41] minimum, with 42-s averaging, the HCHO concentration noise is 8.5 ppt. For the simultaneous HCOOH measurement, the 1-s noise is 50 ppt, and the Allan variance minimum noise at 30 s is 17 ppt. For the simultaneous OCS measurement, the 1-s noise is 9.2 ppt and the Allan variance minimum at 30 s is 2.9 ppt. These results are summarized in Table 2. Although the concentration noise for OCS is better than for HCHO, OCS is a much stronger absorber (∼11x) than HCHO. The absorption noise is therefore lower for the HCHO measurement ($\sim 4.5\times10^{-6}$), compared to the OCS measurement (1.5×10^{-5}).

5 Summary of Results

The measurement of the noise performance of a given instrument is generally straightforward, but the comparison to expectations is much more complex, depending on the dominant noise sources and the measurement time scale. A useful tool for characterizing instrument noise is the Allan variance plot,[41] which shows the variance as a function of averaging time. Usually, the variance will improve as the averaging time (τ) increases (going down as $1/\tau$ for random noise), only until a limiting time, after which the variance will level off or even increase. There are numerous sources of random noise (e.g., laser shot noise, detector noise, amplifier noise) that can contribute to the short-term noise specification. There are also numerous sources of nonrandom noise or drift that may become apparent only at the averaging times where random noise is sufficiently reduced to reveal them. For example, Brownian drift (the integral of random noise) has a variance that increases with averaging time and may dominate the total variance once random noise is sufficiently reduced by averaging.

The total noise in a trace-gas instrument often can be usefully divided into "dark noise," "light noise," and "proportional noise." Dark-noise is the noise seen when the laser light is blocked and includes detector noise and electronic noise. Light noise is the increased noise seen when laser light is present, but without absorbing gases. Light noise sources include laser $1/f$ noise, current supply noise, and interference fringe fluctuations. Proportional noise is seen as the increase in noise when absorbing gases are present and includes such effects as laser frequency instability and linewidth variations. For ARI's trace-gas instruments, the noise ultimately is the variation in the mixing ratio derived from fitting a measured spectrum to a model absorption profile based on HITRAN parameters and other measured quantities. Thus, other sources of noise may appear if, for example, the pressure or temperature measurements have excess noise or if the fit is set up nonoptimally.

Table 3 List of trace gases measured with QCL based instruments at ARI. The top part of the table gives results with pulsed QC lasers, with the 1-s noise scaled to a constant 76-m cell length to give a uniform comparison. The bottom part of the table gives results with CW QCLs, but the noise levels have not been scaled.

		Pulsed Laser	
TRACE GAS	Line (cm^{-1})	1 s rms (ppb) 76-m path	LOD (ppb) 100 s
NH_3	967	0.2	0.06
C_2H_4	960	1	0.5
O_3	1050	1.5	0.6
CH_4	1270	1	0.4
N_2O	1270	0.4	0.2
H_2O_2	1267	3	1
NO_2	1600	0.2	0.1
HONO	1700	0.6	0.3
HNO_3	1723	0.6	0.3
HCHO	1765	0.3	0.15
HCOOH	1765	0.3	0.15
NO	1900	0.6	0.3
OCS	2071	0.06	0.03
CO	2190	0.25	0.1
N_2O	2240	0.2	0.1
$^{13}CO_2/^{12}CO_2$	2311	0.2‰	0.1‰

		CW Laser	LOD (ppt)
TRACE GAS	Line (cm^{-1})	1 s rms (ppb)	100 s
$^{13}CH_4$	1294	25	12
NO_2	1600	10	5
HONO	1659	120	50
NO	1900	40	20
HCHO	1765	32	9
HCOOH	1765	50	17
OCS	2052	5	1
$^{13}CO_2/^{12}CO_2$	2311	0.1‰	0.03‰

Because we have discussed several instruments, we will not present detailed noise analysis for each one, but rather will comment in general on our dominant noise sources, followed by added detail on one instrument. In our pulsed QCL systems, where we operate close to the laser threshold, dark noise tends to dominate the measurement. The new availability of high D^* TE-cooled detectors in the mid-IR allows one to operate with sufficiently low dark noise

Table 4 Noise measurements are shown from various instruments, pulsed and CW, expressed in terms of concentration (ppb), absorption (dimensionless) and as absorbance (normalized by path length). The listed gas concentrations are typical ambient levels.

Gas	Conc. (ppb)	Line (cm^{-1})	Laser Drive	OPL (m)	Absorp. Depth	1-s Noise (ppb)	1-s Noise Absorption	1-s Noise Absorbance (cm^{-1})
N_2O	320	2240	Pulsed	76	0.078	0.25	6.0×10^{-5}	8×10^{-9}
$^{13}CO_2$	3800	2310	Pulsed	7.3	0.12	0.80	2.5×10^{-5}	3×10^{-8}
N_2O	320	2240	CW	76	0.078	0.15	3.6×10^{-5}	5×10^{-9}
OCS	0.5	2040	CW	210	8×10^{-4}	0.0045	7.2×10^{-6}	3.4×10^{-10}
$^{13}CH_4$	18	1294	CW	210	2×10^{-3}	0.025	2.8×10^{-6}	1.3×10^{-10}

for high-sensitivity measurements. We often find that electronic noise can dominate the estimated noise contribution of the detector itself. In our CW laser systems, the laser generally delivers enough power to the detector that the detector noise is not a significant contribution to the total. Electronic noise then dominates the dark noise, but that is seldom the largest noise source. Rather, light noise and proportional noise tend to dominate. Amplitude and frequency noise produced by the laser current driver often is a significant effect. Also, interference fringe instability produces noise and drift on time scales of ~10 to 100 s. Many subtle electronic, control, and thermal effects are revealed as we push to longer averaging times in search of higher precision measurements.

The noise performance for our new dual-laser instrument with the 200-m cell (Fig. 7) illustrates the interplay of several noise sources. The absorption noise levels shown in Table 2, $\sim4.5\times10^{-6}$ for HCHO and $\sim1.5\times10^{-5}$ for OCS (1 standard deviation at 1-s average), result from two lasers multiplexed at 1.1 kHz, with similar powers delivered to the detector. In this case, the absorption depths are so small that proportional noise effects are negligible. The fluctuations in the measured spectra result from dark and light noise effects. Both lasers' spectra are affected by narrowband electronic pickup, which is the major component of the dark noise. The short-term (1s) HCHO concentration noise is close to the darknoise limit, while the OCS noise is approximately three times the dark-noise limit. The short-term (1-s) point-to-point fluctuations in the spectra have (normalized) standard deviations of 4.3×10^{-5} for the HCHO laser and 5.8×10^{-5} for the OCS laser, which are greater than the reported absorption noise levels. The fits effectively average the point-to-point noise over the width of the absorption lines. The final absorption noise can be estimated by convolving the spectral noise with a Gaussian with the appropriate absorption linewidth (four to five channels for these lines), and then subtracting the spectral fluctuations smoothed to a typical baseline width (e.g., 30 channels). The resulting relevant spectral noise levels are 2.6×10^{-6} for the HCHO laser and 8.7×10^{-6} for the OCS laser, which are comparable to the reported absorption noise levels. The excess noise produced by the OCS laser is inherent to the laser and appears to be $1/f$ noise.

The sources of drift in the instrument are distinct from the sources of short-term noise. As seen in the Allan variance plot (Fig. 11), drift dominates the HCHO concentration variations after ~40-s averaging time. In this instrument, an interference fringe with generating length ~70 cm preferentially affects the HCHO spectra, and instability of this fringe is the dominant drift mechanism for HCHO. The 70-cm fringe originates on the optical table and not in the multipass cell. The strongest fringe observed to originate in the cell has a generating length of 10 passes (~470 cm, 0.00213 cm^{-1}), as expected from the pattern selection calculations. This high-frequency cell fringe normally would be expected to have little influence on fits to the wider (~0.02 cm^{-1}) absorption lines. However, in this case the spectral frequency sampling interval is close to the 10-pass fringe period near the OCS line. When the frequency sampling interval nearly matches the fringe spacing, the fringe is "aliased" to lower frequency and can have an unexpectedly large effect on the concentration determination. We have observed such an influence of the 10-pass cell fringe on the OCS concentration, but less so for HCHO because the aliasing does not occur near its line. The influence of the 10-pass cell fringe is minimized by vibration of one of the cell mirrors.

We summarize our recent trace-gas detection results in Tables 3 and 4. In Table 3, we list a set of gases that we have measured with QCL-based instruments, the line position of the absorption line and the measurement noise. Table 3 is divided in two parts, the top showing results with pulsed lasers and the bottom showing results with CW lasers. In the top part of Table 3, the 1-s concentration noise is scaled to a 76 m absorption cell to make a uniform comparison. In the bottom part of Table 3, the noise levels have not been scaled. The final column gives the level of detection at 100-s averaging time.

In Table 4, we show noise results from several instruments, pulsed and CW, presented in terms of concentration, absorption; and as absorbance (normalized by path length). Generally, we achieve significantly improved noise performance with CW lasers compared to pulsed lasers. CW lasers tend to offer higher power, narrower line width, and more symmetrical line shape than pulsed lasers. We operate pulsed lasers close to threshold to reduce line width, which limits its power and may result in more variable pulse energy.[27] Our best absorption noise performance of $\sim3\times10^{-6}$ with a 200-m path length corresponds to an absorbance per unit path length noise of 1.5×10^{-10} cm^{-1}.

6 Conclusions

There are a set of technologies and approaches that contribute to the capability for making high-precision atmospheric trace-gas measurements with QCLs. New CW QCLs are an important advance because they offer higher

power that can compensate for the lower D^* of TE-cooled detectors. Also, CW QCLs offer narrower line width and better stability than pulsed QCLs. We have benefited by the recent availability of higher reflectivity mirrors in the mid-IR, which gives higher throughput multipass cells at high-pass number, and with less scatter for decreased interference fringes. Performance can be further improved with other methods of effectively reducing interference fringes, such as optimum pattern selection in the MPC, mirror vibration, and proper matching into the cell. The availability of more computing power allows more real-time control and allows more signal processing during faster laser sweeps. Improved high-current drivers for QCLs have been important in giving the best noise performance. Techniques to control and stabilize the important physical variables in the instrument, such as temperature and pressure, are crucial for long-term stability. The technique of spectral division has been useful in a variety of ways—to effectively flatten baseline transmission, to remove stable electronic structure, and to reduce the effective absorption depth and thus proportional noise.

The Center for Atmospheric and Environmental Chemistry at ARI was among the first groups to build high-performance QCL-based spectroscopic instrumentation for atmospheric research and to make such instrumentation available to other research groups. Several QCL systems have been developed that show high sensitivity and high pgrecision. Demonstrated absorption noise of ~ 3 to 5×10^{-6} in 1 s leads to concentration noise of ~ 1 to100 ppt, depending on the strength of the absorber and path length. Fractional precision of 1 in 1000 in 1s is routinely achieved for stable gases, when using CW QCLs.

Acknowledgments

We thank Stephan Blaser and Antoine Mueller from ALPES-LASERS for the high-quality QCLs used in this work. Ryan McGovern, Dan Glenn, and Stanley Huang at ARI contributed to the electronic and optical engineering and fabrication. We thank our collaborators on various projects from Harvard University, The University of Arizona, and Empa Laboratory for Air Pollution and Environmental Technology. We thank our instrument customers for helping to bring these new technologies to bear on important real-world problems. Funding for this work has been provided, in part, under the SBIR programs of the Department of Energy, the Department of Commerce, the Environmental Protection Agency, the Department of Agriculture, and by the National Science Foundation.

References

1. J. Faist, F. Capasso, D. L. Sivco, C. Sirtori, A. L. Hutchinson, and A. Y. Cho, "Quantum cascade laser," *Science* **264**, 553–556 (1994).
2. C. Gmachl, F. Capasso, J. Faist, A. L. Hutchinson, A. Tredicucci, D. J. Sivco, J. N. Baillargeon, S. N. G. Chu, and A. Y. Cho, "Continuous-wave and high power pulsed operation of index-coupled distributed feedback quantum cascade laser at $\sim 8.5 \mu$m," *Appl. Phys. Lett.* **72**, 1430–1432 (1998).
3. J. Faist, A. Tredicucci, F. Capasso, C. Sirtori, D. L. Sivco, J. N. Baillargeon, A. L. Hutchinson, and A. Y. Cho, "High-power continuous-wave quantum cascade lasers," *IEEE J. Quantum Electron* **34**, 336–343 (1998).
4. F. Capasso, C. Gmachl, R. Paiella, A. Tredicucci, A. L. Hutchinson, D. L. Sivco, J. N. Baillargeon, A. Y. Cho, and H. C. Liu, "New frontiers in quantum cascade lasers and applications," *IEEE J. Sel. Top. Quantum Electron* **6**, 931–947 (2000).
5. C. Gmachl, F. Capasso, D. L. Sivco, and A. Y. Cho, "Recent progress in quantum cascade lasers and applications," *Rep. Prog. Phys.* **64**, 1533–1601 (2001).
6. M. Beck, D. Hofstetter, T. Aellen, J. Faist, U. Oesterle, M. Ilegems, E. Gini, and H. Melchior, "Continuous wave operation of a mid-infrared semiconductor laser at room temperature," *Science* **295**, 301–305 (2002).
7. R. F. Curl, F. Capasso, C. Gmachl, A. A. Kosterev, J. B. McManus, R. Lewicki, M. Pusharsky, G. Wysocki, and F. K. Tittel, "Quantum cascade lasers in chemical physics," *Chem. Phys. Lett.* **487**, 1–18 (2010).
8. F. K. Tittel, Y. Bakhirkin, A. A. Kosterev, and G. Wysocki, "Recent advances in trace gas detection using quantum and interband cascade lasers," *Rev. Laser Eng.* **34**, 275–282 (2006).
9. C. R. Webster, G. J. Flesch, D. C. Scott, J. E. Swanson, R. D. May, W. S. Woodward, C. Gmachl, F. Capasso, D. L. Sivco, J. N. Baillargeon, A. L. Hutchinson, and A. Y. Cho, "Quantum-cascade laser measurements of stratospheric methane and nitrous oxide," *Appl. Opt.* **40**, 321–326 (2001).
10. C. L. Schiller, H. Bozem, C. Gurk, U. Parchatka, R. Königstedt, G. W. Harris, J. Lelieveld, and H. Fisher, "Applications of quantum cascade lasers for sensitive trace gas measurements of CO, CH_4, N_2O, and HCHO," *Appl. Phys. B* **92**, 419–430 (2008).
11. A. A. Kosterev, F. K. Tittel, R. Köhler, C. Gmachl, F. Capasso, D. L. Sivco, A. Y. Cho, S. Wehe, and M. G. Allen, "Thermoelectrically cooled quantum-cascade laser-based sensor for the continuous monitoring of ambient atmospheric carbon monoxide," *Appl. Opt.* **41**, 1169–1173 (2002).
12. W. H. Weber, J. T. Remillard, R. E. Chase, J. F. Richert, F. Capasso, C. Gmachl, A. L. Hutchinson, D. L. Sivco, J. N. Baillargeon, and A. Y. Cho, "Using a wavelength-modulated quantum cascade laser to measure NO Concentrations in the parts-per-billion range for vehicle emissions certification," *Appl. Spectrosc.* **56**, 706–714 (2002).
13. A. A. Kosterev, R. F. Curl, F. K. Tittel, R. Köhler, C. Gmachl, F. Capasso, D. L. Sivco, and A. Y. Cho, "Transported automated ammonia sensor based on a pulsed thermoelectrically cooled QC-DFB laser," *Appl. Opt.* **41**, 573–578 (2002).
14. A. A. Kosterev and F. K. Tittel, "Chemical sensors based on quantum cascade lasers," *IEEE Quantum Electron* **38**, 582–591 (2002).
15. D. D. Nelson, J. H. Shorter, J. B. McManus, and M. S. Zahniser, "Sub-part-per-billion detection of nitric oxide in air using a thermoelectrically cooled mid-infrared quantum cascade laser spectrometer," *Appl. Phys. B* **75**, 343–350 (2002).
16. J. B. McManus, D. D. Nelson, J. H. Shorter, and M. S. Zahniser, "Quantum cascade lasers for open- and closed-path measurement of atmospheric trace gases," *Proc. SPIE* **4817**, 22–33 (2002).
17. D. D. Nelson, J. B. McManus, S. Urbanski, S. Herndon, and M. S. Zahniser, "High precision measurements of atmospheric nitrous oxide and methane using thermoelectrically cooled mid-infrared quantum cascade lasers and detectors," *Spectrochim. Acta A* **60**, 3325–3335 (2004).
18. R. Jimenez, S. Herndon, J. H. Shorter, D. D. Nelson, J. B. McManus, and M. S. Zahniser, "Atmospheric trace gas measurements using a dual quantum-cascade laser mid-Infrared absorption spectrometer," *Proc. SPIE* **5738**, 318–330 (2005).
19. S. C. Herndon, M. S. Zahniser, D. D. Nelson, J. H. Shorter, J. B. McManus, R. Jiménez, C. Warneke, and J. A. de Gouw, "Airborne measurements of HCHO and HCOOH during the New England Air Quality Study 2004 using a pulsed quantum cascade laser spectrometer," *J. Geophys. Res.* **112**(D10), D10S03 (2007).
20. P. M. Chu, D. D. Nelson, M. S. Zahniser, J. B. McManus, Q. Shi, and J. C. Travis, "Towards realization of reactive gas amount of substance standards through spectroscopic measurements," *IEEE Trans. Instrum. Meas.* **56**, 305–308 (2007).
21. J. B. McManus, J. H. Shorter, D. D. Nelson, M. S. Zahniser, D. E. Glenn, and R. M. McGovern, "Pulsed quantum cascade laser instrument with compact design for rapid, high sensitivity measurements of trace gases in air," *Appl. Phys. B* **92**, 387–392 (2008).
22. D. D. Nelson, J. B. McManus, S. C. Herndon, M. S. Zahniser, B. Tuzson, and L. Emmenegger, "New method for isotopic ratio measurements of atmospheric carbon dioxide using a 4.3 μm pulsed quantum cascade laser," *Appl. Phys. B* **90**, 301–309 (2008).
23. B. Tuzson, J. Mohn, M. J. Zeeman, R. A. Werner, W. Eugster, M. S. Zahniser, D. D. Nelson, J. B. McManus and L. Emmenegger, "High precision and continuous field measurements of $\delta^{13}C$ and $\delta^{18}O$ in carbon dioxide with a cryogen-free QCLAS," *Appl. Phys. B* **90**, 415–458 (2008).
24. J. B. McManus, D. D. Nelson, and M. S. Zahniser, "Long-term continuous sampling of $^{12}CO_2$, $^{13}CO_2$ and $^{12}C^{18}O^{16}O$ in ambient air with a quantum cascade laser spectrometer," *Isotopes Environ. Health Stud.* **46**, 49–63 (2010).
25. M. S. Zahniser, D. D. Nelson, J. B. McManus, S. Herndon, E. Wood, J. H. Shorter, B. Lee, G. Santoni, R. Jimenez, and B. Daube, "Infrared QC laser applications to field measurements of atmospheric trace gas sources and sinks in environmental research: enhanced

capabilities using continuous wave QCLs," *Proc. SPIE* **7222**, 72220H (2009).
26. D. D. Nelson, J. B. McManus, S. C. Herndon, J. H. Shorter, M. S. Zahniser, S. Blaser, L. Hvozdara, A. Muller, M. Giovannini, and J. Faist, "Characterization of a near-room temperature, continuous-wave quantum cascade laser for long-term, unattended monitoring of nitric oxide in the atmosphere," *Opt. Lett.* **31**, 2012–2014 (2006).
27. J. B. McManus, D. D. Nelson, S. C. Herndon, J. H. Shorter, M. S. Zahniser, S. Blaser, L. Hvozdara, A. Muller, M. Giovannini, and J. Faist "Comparison of CW and pulsed operation with a TE-cooled quantum cascade infrared laser for detection of nitric oxide at 1900 cm^{-1}," *Appl. Phys. B* **85**, 235–241 (2006).
28. P. Werle, "A review of recent advances in semiconductor laser based gas monitors," *Spectrochim. Acta A* **54**, 197–236 (1998).
29. F. K. Tittel, D. Richter, and A. Fried, "Mid-infrared laser applications in spectroscopy," in *Topics in Applied Physics* Vol. 89, I. T. Sorokina and K. L. Vodopyanov, Eds., pp. 445–516, Springer-Verlag, Berlin, (2003).
30. J. B. McManus, "Paraxial matrix description of astigmatic and cylindrical mirror resonators with twisted axes for laser spectroscopy," *Appl. Opt.* **46**, 472–482 (2007).
31. J. B. McManus, P. L Kebabian, and M. S. Zahniser, "Astigmatic mirror multiple pass absorption cells for long pathlength spectroscopy," *Appl. Opt.* **34**, 3336–3348 (1995).
32. L. S. Rothman, A. Barbe, D. Chris Benner, L. R. Brown, C. Camy-Peyret, M. R. Carleer, K. Chance, C. Clerbaux, V. Dana, V. M. Devi, A. Fayt, J.-M. Flaud, R. R. Gamache, A. Goldman, D. Jacquemart, K. W. Jucks, M. J. Lafferty, J. Y. Mandin, S. T. Massie, V. Nemtchinov, D. A. Newnham, A. Perrin, C. P. Rinsland, J. Schroeder, K. M. Smith, M. A. H. Smith, K. Tang, R. A. Toth, J. Vander Auwera, P. Varanasi, and K. Yoshino, "The HITRAN molecular spectroscopic database: edition of 2000 with updates through 2001," *J. Quantum Spectrosc. Radiat. Transfer* **82**, 5–44 (2003).
33. S. C. Wofsy, B. Daube, R. Jimenez, S. Park, and E. A. Kort, "Measurements of atmospheric CO_2, CH_4, CO and N_2O from the HIAPER GV aircraft in April–June 2008," American Geophysical Union, Fall Meeting 2008, EOS Trans **89**, abstract A43F-01.
34. A. Fried, Y. Wang, C. Cantrell, B. Wert, J. Walega, B. Ridley, E. Atlas, R. Shetter, B. Lefer, M. T. Coffey, J. Hannigan, D. Blake, N. Blake, S. Meinardi, B. Talbot, J. Dibb, E. Scheuer, O. Wingenter, J. Snow, B. Heikes, and D. Ehhalt, "Tunable diode laser measurements of formaldehdye during the TOPSE 2000: Distributions, trends, and model comparisons," *J. Geophys. Res.* **108**(D4), 8365 (2003).
35. D. Richter, A. Fried, B. P. Wert, J. G. Walega, and F. K. Tittel, "Development of a tunable mid-IR difference-frequency laser source for highly sensitive airborne trace gas detection," *Appl. Phys. B* **75**, 281–288 (2002).
36. Y. Q. Li, K. L. Demerjian, M. S. Zahniser, D. D. Nelson, J. B. McManus, and S. C. Herndon, "Measurement of formaldehyde, nitrogen dioxide, and sulfur dioxide at Whiteface Mountain using a dual tunable diode laser system," *J. Geophys. Res.* **109**, D16S08 (2004).
37. G. Wysocki, Y. Bakhirkin, S. So, F. K. Tittel, C. J. Hill, R. Q. Yang, and M. P. Fraser, "Dual interband cascade laser based trace-gas sensor for environmental monitoring," *Appl. Opt.* **46**, 8202–8210 (2007).
38. K. Stimler, D. Nelson, and D. Yakir, "High precision measurements of atmospheric concentrations and plant exchange rates of carbonyl sulfide (COS) using mid-IR quantum cascade laser," *Global Change Bio.* **16**, 2496–2503 (2010).
39. A. Fried, J. R. Drummond, B. Henry, and J. Fox, "Versatile integrated tunable diode laser system for high precision: application for ambient measurements of OCS," *Appl. Opt.* **30**, 1916–1932 (1991).
40. G. Wysocki, M. McCurdy, S. So, D. Weidmann, C. Roller, R. F. Curl, and F. K. Tittel, "Pulsed quantum-cascade laser-based sensor for trace-gas detection of carbonyl sulfide," *Appl. Opt.* **43**, 6040–6046 (2004).
41. P. Werle, R. Mucke, and F. Slemr, "The limits of signal averaging in atmospheric trace-gas monitoring by tunable diode-laser absorption spectroscopy (TDLAS)," *Appl. Phys. B* **57**, 131–139 (1993).

J. Barry McManus received his PhD in physics from Massachusetts Institute of Technology, Cambridge, Massachusetts, in 1982. Since 1986, he has been with ARI, Billerica, Massachusetts, where he is currently in the Center for Atmospheric and Environmental Chemistry. He is focused primarily on the development of laser spectroscopic instrumentation for environmental and atmospheric research. Dr. McManus is a fellow of the Optical Society of America.

Mark S. Zahniser received his PhD in physical chemistry from the University of Pittsburg, Pittsburg, Pennsylvania in 1977. He joined ARI, Billerica, Massachusetts in 1979, where he currently leads the Center for Atmospheric and Environmental Chemistry. He is active in developing methods for *in situ* monitoring of trace gas fluxes using laser spectroscopy.

David D. Nelson, Jr. received his PhD in chemical physics from Harvard University, Cambridge, Massachusetts in 1987. He joined ARI, Billerica, Massachusetts in 1989, and since 1997, has been the director of Aerodyne's Technical Facilities. His research interests include gas-phase chemical kinetics, atmospheric chemistry, and applied laser spectroscopy, including the development of laser-based field instruments for detection of trace atmospheric species. Dr. Nelson is a fellow of the Optical Society of America.

Joanne H. Shorter received her PhD in physical chemistry from Massachusetts Institute of Technology, Cambridge, Massachusetts in 1990. Since 1991 she has been at ARI, Billerica, Massachusetts, where she is currently in the Center for Atmospheric and Environmental Chemistry. Her research interests include the development of laser-based sensors for atmospheric, environmental, and medical applications.

Scott Herndon received his PhD in chemistry and biochemistry from the University of Colorado in 1999. Since 1991 he has been at ARI, Billerica, Massachusetts, where he is currently in the Center for Atmospheric and Environmental Chemistry. His research interests include atmospheric chemistry, trace gas emissions measurements, and development of laser-based sensors for atmospheric and environmental applications.

Ezra Wood received his PhD in chemistry from the University of California, Berkeley in 2004. Since 2006, he has been at ARI, Billerica, Massachusetts, where he is currently in the Center for Atmospheric and Environmental Chemistry. His research interests include atmospheric chemistry and trace gas emissions measurements.

Rick Wehr: biography not available.